A Kirkwood–Buff derived force field for sodium chloride in water

Samantha Weerasinghe and Paul E. Smith

Citation: J. Chem. Phys. **119**, 11342 (2003); doi: 10.1063/1.1622372
View online: http://dx.doi.org/10.1063/1.1622372
View Table of Contents: http://jcp.aip.org/resource/1/JCPSA6/v119/i21
Published by the American Institute of Physics.

A Kirkwood–Buff derived force field for sodium chloride in water

Samantha Weerasinghe[a] and Paul E. Smith[b]
Department of Chemistry, Kansas State University, Manhattan, Kansas 66506-3701

(Received 6 August 2003; accepted 4 September 2003)

A force field for the simulation of mixtures of sodium chloride and water is described. The model is specifically designed to reproduce the experimentally determined Kirkwood–Buff integrals as a function of salt concentration, ensuring that a good representation of the solution activity is obtained. In addition, the model reproduces many of the known properties of sodium chloride solutions including the density, isothermal compressibility, ion diffusion constants, relative permittivity, and the heat of mixing. The results are also compared to other common sodium chloride force fields. © *2003 American Institute of Physics.* [DOI: 10.1063/1.1622372]

INTRODUCTION

The choice of force field is critical for a correct description of any particular system by computer simulation. The accuracy of a force field is usually determined by comparison with a range of experimentally determined physical and thermodynamic properties. It is therefore surprising that parameters developed for the description of sodium chloride solutions vary so widely between different force fields.[1] This arises, at least in part, from the fact that salt solutions are particularly difficult to parametrize as one typically has more parameters (two σ and two ε for the common Lennard-Jones plus Coulomb potential) than experimental data which is sensitive to these parameters (such as the density or ion diffusion constants).

Recently, we have been developing a force field (KBFF) for molecular dynamics (MD) simulations which is specifically designed to reproduce Kirkwood–Buff (KB) integrals obtained from the experimental data (activity coefficients, density, and compressibility) on solution mixtures.[2,3] This approach has several advantages. First, a KB analysis provides more data for testing of the force field. Second, one has access to the activity which represents the most fundamental thermodynamic property of a solution mixture. Third, KB integrals have been shown to be a sensitive probe of the molecular distributions observed for different solutions and can be used to distinguish between models with otherwise similar characteristics. It has also been demonstrated that many of the common force fields currently in use do not necessarily reproduce the correct solution activities,[4,5] and that this can lead to inaccurate simulation data concerning the preferential interaction of cosolvents with solutes in solution.[5] Here, a KB analysis of the properties of sodium chloride solutions as a function of salt concentration is used to guide the development of a force field for the description of sodium chloride solutions using the extended simple point charge (SPC/E) water model.

The model used here does not include explicit polarization effects as it is designed to be used for the study of salt effects on peptides, proteins or DNA. Polarizable force fields for biological systems are still in their infancy and hence there is still the need for accurate complementary nonpolarizable models. For this reason we also compare our results to those generated by the sodium chloride parameters included in some of the common protein force fields presently in use.

METHODS

Kirkwood–Buff theory

The development of KB theory is described in detail elsewhere.[6,7] The thermodynamic properties of a solution mixture can be expressed in terms of the KB integrals between the different solution components which are defined as[7]

$$G_{ij}=4\pi\int_0^\infty [g_{ij}^{\mu VT}(r)-1]r^2\,dr. \tag{1}$$

Here, G_{ij} is the KB integral between species i and j, $g_{ij}^{\mu VT}(r)$ is the corresponding radial distribution function (rdf) in the μVT ensemble, and r is the corresponding center-of-mass to center-of-mass distance. KB integrals were determined from the simulation data (NpT ensemble) by assuming that,[6,8–10]

$$G_{ij}(R)=4\pi\int_0^R [g_{ij}^{NpT}(r)-1]r^2\,dr, \tag{2}$$

where R represents a correlation region within which the solution composition differs from the bulk composition.[6] All rdfs are assumed to be unity beyond R. Excess coordination numbers are defined as $N_{ij}=\rho_j G_{ij}$, where $\rho_j=N_j/V$ is the number density of j particles. A value of N_{ij} greater than zero indicates an excess of species j in the vicinity of species i (over a random distribution), while a negative value corresponds to a depletion of species j surrounding i.

For a binary solution consisting of water (w) and a cosolvent (c), a variety of thermodynamic quantities can be defined in terms of the KB integrals G_{ww}, G_{cc}, and $G_{cw}=G_{wc}$, and the number densities (or molar concentrations) ρ_w and ρ_c. The partial molar volumes of the components

[a]Permanent address: Department of Chemistry, University of Ruhuna, Matara, Sri Lanka.
[b]Electronic mail: pesmith@ksu.edu

($\overline{V}_i$) and the derivative of the cosolvent activity ($a_c = y_c \rho_c$) at a pressure (p) and a temperature (T) are given by[6]

$$\overline{V}_w = \frac{1+\rho_c(G_{cc}-G_{cw})}{\eta}, \quad \overline{V}_c = \frac{1+\rho_w(G_{ww}-G_{cw})}{\eta}, \tag{3}$$

$$a_{cc} = \left(\frac{\partial \ln a_c}{\partial \ln \rho_c}\right)_{p,T} = 1 + \left(\frac{\partial \ln y_c}{\partial \ln \rho_c}\right)_{p,T} = \frac{1}{1+\rho_c(G_{cc}-G_{cw})}, \tag{4}$$

where $\eta = \rho_w + \rho_c + \rho_w \rho_c (G_{ww} + G_{cc} - 2G_{cw})$. There are no approximations made during the derivation of the above equations.[7] Our previous simulations and others have indicated that a combination of KB theory and *NpT* simulations can provide quantitative information concerning the thermodynamics of solutions.[4,8,11,12]

A slight complication arises when applying KB theory to the study of salt solutions. As a result of electroneutrality conditions, it is not possible to consider the salt solution as a ternary system of cations, anions, and water, i.e., one cannot obtain derivatives of the sodium or chloride ion chemical potentials or activities.[13] However, it is possible to treat the salt solution as a binary system of indistinguishable ions and water. This point has been discussed in detail elsewhere.[9,13–15] Hence, we shall distinguish between the cosolvent (total ion) concentration, ρ_c, and the classical salt concentration, C_s. Consequently, for a 1:1 salt one has $\rho_c = 2C_s$, $\overline{V}_s = 2\overline{V}_c$, and $y_c = y_\pm$. In addition, the following relationships are also obeyed, $\rho_c \overline{V}_c + \rho_w \overline{V}_w = 1$ and $\rho_c \mathrm{d} \ln a_c + \rho_w \mathrm{d} \ln a_w = 0$, at constant p and T.

A Kirkwood–Buff analysis of the experimental data at 300 K and 1 atm was recently performed[9] using two different sources for the activity of sodium chloride solutions,[16,17] combined with the density and compressibility data.[18] As the activities are typically the largest source of error in the KB analysis,[19] we have included both sets of data in our comparison to provide an estimate of the degree of uncertainty in the experimentally derived KB integrals. Where only one experimental KB value is presented the data corresponds to an analysis using the Robinson and Stokes activities.[16]

Molecular dynamics simulations

All sodium chloride solutions were simulated using classical molecular dynamics techniques. Several water models were used (SPC/E, SPC, and TIP3P), although the majority of simulations involved the SPC/E model. All simulations were performed in the isothermal isobaric ensemble at 300 K and 1 atm. The weak coupling technique[20] was used to modulate the temperature and pressure with relaxation times of 0.1 and 0.5 ps, respectively. All bonds were constrained using SHAKE[21] and a relative tolerance of 10^{-4}, allowing a 2 fs time step for integration of the equations of motion. The particle mesh Ewald technique was used to evaluate electrostatic interactions.[22,23] A real space convergence parameter of 3.5 nm^{-1} was used in combination with twin range cutoffs of 0.8 and 1.2 nm, and a nonbonded update frequency of 10 steps. The reciprocal space sum was evaluated on a 40^3 grid with $\approx$0.1 nm resolution. Initial configurations of the different solutions were generated from a cubic box ($L \approx 4.0$ nm) of equilibrated water molecules by randomly replacing waters and/or inserting ions until the required concentration was attained. The steepest descent method was then used to perform 100 steps of minimization. This was followed by extensive equilibration which was continued until all intermolecular potential energy contributions displayed no drift with time (typically 1 ns). Configurations were saved every 0.1 ps for analysis. Diffusion constants were determined using the mean square fluctuation approach,[24] relative permittivities from the dipole moment fluctuations,[25] and finite difference compressibilities by performing additional simulations of 250 ps at 1000 atm. The excess enthalpy of mixing (ΔH_m) was determined using an established procedure,[26] with configurational energies for pure SPC/E water, pure SPC water, and the sodium chloride lattice of -46.45, 41.60, and -808.24 kJ/mol, respectively. Errors ($\pm 1\sigma$) in the simulation data were estimated by using two or three block averages.

Parameter development

The force field used in this study corresponded to the Lennard-Jones (LJ) 6-12 plus Coulomb potential, which is the most commonly used potential for biomolecular simulation. In this scheme each pair of atoms i and j interact with an interaction energy given by

$$V_{ij} = \frac{q_i q_j}{4\pi\varepsilon_o r_{ij}} + 4\varepsilon_{ij}\left[\left(\frac{\sigma_{ij}}{r_{ij}}\right)^{12} - \left(\frac{\sigma_{ij}}{r_{ij}}\right)^{6}\right], \tag{5}$$

where all the symbols have their usual meaning.[27] Our previous studies used a simple scheme to obtain parameters for the LJ term.[2,3] The charges on the atoms were then adjusted to reproduce the density and KB integrals. This is not possible for simple monoatomic salt ions. Hence, we have adopted a different approach. In an effort to ensure the ions are of the correct size we have used three pieces of experimental data to guide our parameter development. These are the ionic radii of sodium (0.101 nm) and chloride (0.181 nm) ions which are consistent with the crystal lattice dimensions,[28] the crystal lattice unit cell dimension of 0.282 nm,[29] and the ion to water oxygen contact distances of 0.24 and 0.32 nm for sodium and chloride ions in solution, respectively.[28]

The final parameters were obtained from a three step process. First, the values of σ_{++} and σ_{--} were determined by assuming $\varepsilon_{++} = \varepsilon_{--} = 0.5$ kJ/mol and scaling the ionic radii until the sodium chloride lattice dimensions were reproduced by simulation. The final scaling factor was 2.43. Second, using the values of σ_{++} and σ_{--} obtained from step one a simulation of a 4 M sodium chloride solution was then performed and the ε_{++} and ε_{--} parameters varied independently to reproduce the ion to water oxygen contact distances. Finally, the KB integrals obtained from the simulation of 4 M sodium chloride were compared to the experimental data. Unfortunately, it was not possible to fit the KB data without breaking the geometric combination

TABLE I. Nonbonded parameters. Lennard-Jones 6-12 plus Coulomb potential. Geometric mean combination rules were used for ε_{ij}. Geometric mean combination rules for σ_{ij} were used for the KBFF, GROMOS (43A1), and AMBER (ff98) force fields. Arithmetic mean combination rules for σ_{ij} were used for the CHARMM (v27) force field. A scaling factor of 0.75 was applied to the ε_{ij} between sodium and water oxygen for the KBFF model ($\varepsilon_{+o}=0.342$ kJ/mol).

Model	Atom	ε (kJ/mol)	σ (nm)	q ($\lvert e\rvert$)	References
KBFF	Na^+	0.320	0.245	1.0	
	Cl^-	0.470	0.440	−1.0	
GROMOS	Na^+	0.062	0.258	1.0	34
	Cl^-	0.446	0.445	−1.0	
AMBER	Na^+	0.012	0.333	1.0	35
	Cl^-	0.418	0.440	−1.0	
CHARMM	Na^+	0.196	0.243	1.0	36
	Cl^-	0.628	0.405	−1.0	
SPC/E	O	0.6506	0.3166	−0.8476	37
	H	0.00	0.00	0.4238	
SPC	O	0.6506	0.3166	−0.82	38
	H	0.0	0.0	0.41	
TIP3P	O	0.6364	0.3151	−0.834	39
	H	0.0	0.0	0.417	

rule for ε parameters between the ions and water oxygen. When the combination rule was used the value of G_{cc} was always positive, whereas the experimental data indicates a value of -54 cm^3/mol for 4 M sodium chloride solutions.[9] Further tests suggested the KB data was more sensitive to changes in the ε_{+o} parameter than the ε_{-o} parameter. Therefore, a simple scaling of the ε_{+o} parameter was used to fit the data, with a scaling factor of 0.75 producing good results. The final parameters used in this study are presented in Table I.

RESULTS

A series of molecular dynamics simulations of sodium chloride solutions were performed and are summarized in Table II. A simulation of the NaCl crystal resulted in a unit cell distance and lattice energy of 0.285 nm and −808 kJ/mol compared to the experimental values of 0.282 nm and −764 kJ/mol, respectively.[29,30] The agreement is reasonable for a simple Coulomb plus Lennard-Jones 6-12 potential.[1] The rdfs obtained from the 1 M and 4 M simulations are displayed in Fig. 1. The high solvation of both ions was evident in a large first peak in the ion to water oxygen rdfs. The peak positions of 0.23 and 0.32 nm for the sodium and chloride ions agree well with the experimental values of 0.24 and 0.32 nm, respectively.[28] Of course, this data was used during the parametrization procedure. The sodium to chloride rdf displayed a large first and a significant second peak which were somewhat concentration dependent. The corresponding first shell coordination numbers are displayed in Table III. The ion to water coordination numbers for sodium and chloride were within the range of experimentally observed values.[28] The variation of coordination number with salt concentration followed the expected trends except for the chloride water coordination number which increased as the salt concentration increased. Also noticeable was a large increase in chloride-to-chloride ion pairing. This was consistent with water mediated chloride-to-chloride ion pairing,

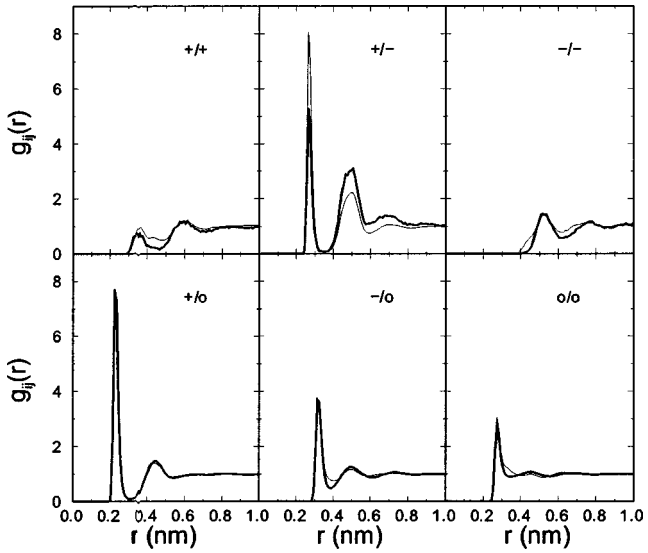

FIG. 1. Radial distribution functions obtained from the 1 M (thick lines) and 4 M (thin lines) simulations. Cations, anions, and the water oxygen are denoted by the symbols +, −, and *o*, respectively.

TABLE II. Summary of the MD simulations of NaCl/water mixtures. All simulations were performed at 300 K and 1 atm in the *NpT* ensemble. Symbols are N_w, number of water molecules; $N_s(=N_+=N_-=\frac{1}{2}N_c)$, number of sodium−chloride pairs; V, average simulation volume; m_s, salt molality; id, infinite dilution; C_s, salt molarity; ρ, mass density; E_{pol}, average total potential energy per molecule (N_s+N_w); and T_{sim}, total simulation time.

N_s	N_w	m_s (mol/Kg)	V (nm^3)	C_s (mol/l)	ρ (g/cm^3)	E_{pot} (kJ/mol)	T_{sim} (ns)
0	2170	0.00	65.265	0.00	0.995	−46.45	2.0
1	2168	id	65.408			−46.74	0.5
20	2150	0.52	65.278	0.51	1.015	−53.42	9.0
38	2079	1.01	63.595	0.99	1.036	−60.07	6.0
77	2048	2.09	63.829	2.00	1.077	−73.99	4.0
115	1987	3.21	63.354	3.01	1.114	−88.00	4.0
154	1950	4.38	63.783	4.01	1.149	−102.02	4.0
1372	0		63.163		2.108	−808.24	0.5

TABLE III. First shell coordination numbers (n_{ij}) for NaCl/water mixtures. $R_{\max}$ and $R_{\min}$ are the distances (nm) to the first maximum and minimum of the rdf, respectively, Sodium cations, anions, and water oxygen are denoted by +, −, and *o*, respectively.

				C_s				
	$R_{\max}$	$R_{\min}$	id	0.5	1.0	2.0	3.0	4.0
n_{++}	0.36	0.450		0.02	0.07	0.18	0.29	0.44
n_{+-}	0.27	0.355		0.06	0.09	0.20	0.42	0.57
n_{--}	0.52	0.615		0.13	0.34	0.65	1.10	1.65
n_{+o}	0.23	0.315	5.63	5.55	5.52	5.39	5.11	4.93
n_{-o}	0.32	0.405	8.23	8.05	8.11	8.22	8.38	8.45
n_{oo}	0.28	0.345	5.11	5.11	5.12	5.11	5.06	5.00

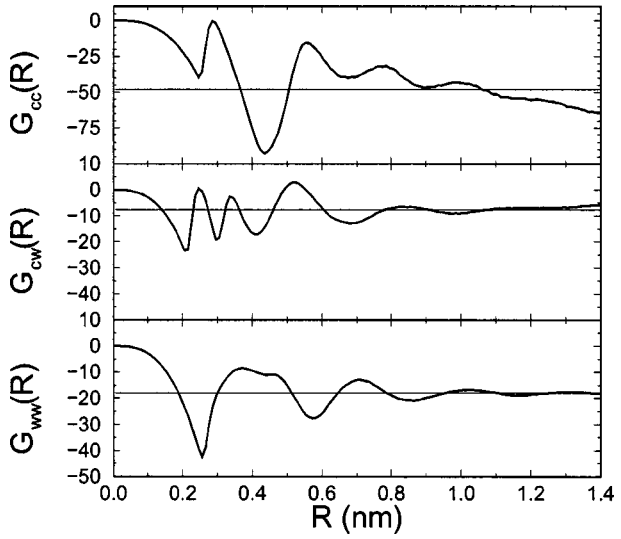

FIG. 2. Kirkwood–Buff integrals (cm^3/mol) as a function of integration distance (R) obtained from the 4 M simulation. The thin horizontal lines correspond to the values obtained after averaging $G_{ij}(R)$ between 0.85 and 1.2 nm.

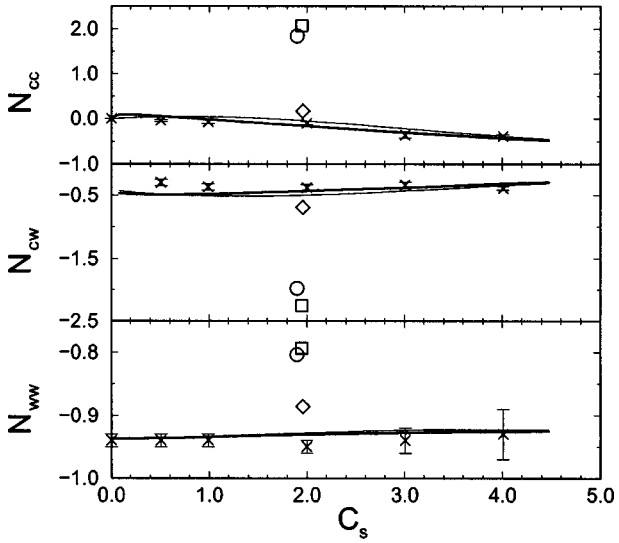

FIG. 3. Excess coordination numbers as a function of molar salt concentration. The thick and thin lines correspond to a KB analysis using two different experimental activity determinations (Ref. 9). The crosses are the results for the KBFF parametrization, while the square, circle, and diamond correspond to the AMBER, GROMOS, and CHARMM force fields, respectively.

which became more favorable with increasing salt concentration to an extent that at 3 M salt a chloride ion was, on the average, paired with another chloride ion.

The KB integrals as a function of integration distance obtained from the 4 M simulation are displayed in Fig. 2. The KB integrals should reach a plateau value at the distance that the rdfs tend towards unity. This was evident for G_{cw} and G_{ww}, but not so convincing for G_{cc}. The latter value suffers from lower sampling as one has far fewer cosolvent ions than water molecules. Following our earlier work,[2,3] the average of the KB integrals between 0.85 and 1.20 nm, representing approximately one oscillation in the functions, was used as the final simulated value of the integrals. This is a somewhat arbitrary procedure but does capture the significant differences in the degree of molecular association in solution between different cosolvent models.

The resulting KB integrals as a function of salt concentration are displayed in Fig. 3 as excess coordination numbers (N_{ij}). The KBFF model reproduced the experimental data very successfully. In comparison, the other NaCl force fields did not. In fact, many force fields displayed both the wrong sign for G_{cc} and an order of magnitude error in the degree of ion self-association. Consequently, the derivative of the molar activity coefficient with concentration displays the wrong sign (negative instead of positive) and the activity coefficient will decrease instead of increase with concentration. This point is further illustrated in Table IV where a comparison of different models is presented for the 2 M simulations. Only the KBFF predicted the correct sign for G_{cc}. More importantly, these results demonstrate that not only can a KB analysis of simulated cosolvent solutions provide further data for comparison with experiment, but it can be used as a sensitive tool for distinguishing between different models which otherwise display similar densities and diffusion constants.

As mentioned previously, one cannot consider a salt solution as a ternary system of sodium ions, chloride ions, and water molecules. However, it is still possible to extract ion–ion KB integrals. From the electroneutrality conditions for a 1:1 salt one can show that $\rho_c G_{+-} = 1 + \rho_c G_{cc}$ and $\rho_+ G_{++} - \rho_- G_{+-} = -1$.[9] Using the simulated value of $\rho_c G_{cc} = -0.38$ for the 4 M solution resulted in a value of $\rho_+ G_{+-} = \rho_- G_{+-} = 0.31$, which is in good agreement with the experimental value of 0.28. Furthermore, $\rho_+ G_{++} = \rho_- G_{--} = -0.69$, compared to the experimental value of -0.72. These integral values provide a different view of ion pairing in solution than that provided by the first shell coordination numbers presented in Table III. The coordination numbers indicated a high degree of chloride-to-chloride ion pairing, probably solvent separated ion pairing. On the other hand, the KB integrals suggested a net depletion of chloride ions around other chloride ions. This is, of course, due to the inclusion of the ion distribution beyond the first shell in the KB integral values. However, it does highlight the fact that

TABLE IV. Comparison of the properties of a 2 M NaCl solution obtained with different force fields. All simulations were performed for 2 ns at 300 K and 1 atm using 77 sodium chlorides and 2048 water molecules, and the parameters from Table I. Experimental data, density from Ref. 18; diffusion coefficients from Ref. 31; and KB integrals from Ref. 9.

	KBFF SPC/E	GROMOS SPC	CHARMM TIP3P	AMBER TIP3P	Expt.	Units
ρ	1.077	1.020	1.052	1.048	1.075	g/cm^3
C_s	2.00	1.90	1.95	1.95	2.00	mol/l
D_+	0.9	1.7	1.6	1.3	1.13	10^{-9} m^2/s
D_-	1.1	1.8	1.9	1.6	1.66	10^{-9} m^2/s
D_w	2.18	5.60	3.93	4.38		10^{-9} m^2/s
$\overline{V}_s$	17.0	27.6	24.2	27.8	20.8	cm^3/mol
$\overline{V}_w$	18.1	18.9	18.3	18.2	18.0	cm^3/mol
G_{cc}	−25	482	43	530	−42	cm^3/mol
G_{ww}	−18	−16	−17	−15	−18	cm^3/mol
G_{cw}	−7	−39	−13	−43	−8	cm^3/mol
a_{cc}	1.08	0.34	0.82	0.31	1.15	

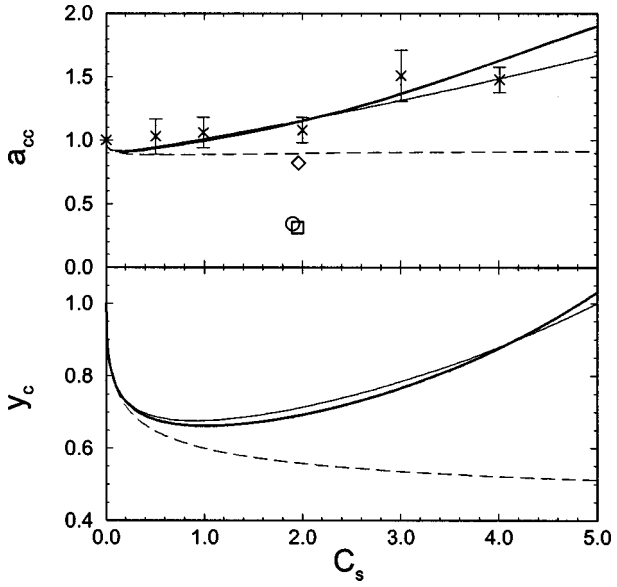

FIG. 4. Activity derivative (top) and molar activity coefficient (bottom) as a function of molar salt concentration. The thick lines represent the experimental data (Refs. 9 and 16), while the thin lines were obtained from a fit of the derivative of Eq. (6) to the simulated derivatives. The dashed lines correspond to the contribution of the first term on the right-hand side of Eq. (6). The crosses are the results for the KBFF parametrization, while the square, circle, and diamond correspond to the AMBER, GROMOS, and CHARMM force fields, respectively.

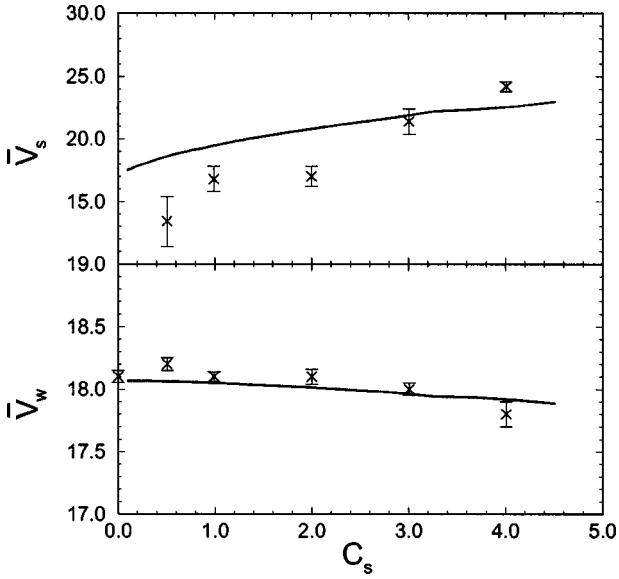

FIG. 5. Partial molar volumes (cm^3/mol) as a function of molar salt concentration. Lines represent the experimental data (Refs. 9 and 18) and crosses correspond to the KBFF model.

first shell coordination numbers do not necessarily directly relate to the overall properties of the solution.

One of the advantages of analyzing the simulation data using KB theory is the information provided concerning the solution activity. In Fig. 4 the simulated activity derivatives a_{cc} as a function of salt concentration are compared to the experimental values. The KBFF model reproduced the correct increase in a_{cc} with concentration displayed by the experimental data. This was not true for all salt models. An expression for the molar activity coefficient ($y_c = y_\pm$) was obtained by extending the fitting equations described in Robinson and Stokes (pp. 229–236 of Ref. 16) so that for a 1:1 salt one has,

$$\ln y_c = -\frac{1.184\sqrt{C_s}}{1+1.32\sqrt{C_s}} + aC_s + bC_s^2, \tag{6}$$

where the first term on the right-hand side has been chosen to reproduce the experimental activity coefficient at low (<0.1 M) concentrations. This was necessary as a KB analysis of such low concentrations of salt is currently statistically unreliable. Using the above expression an equation for a_{cc} can be generated and the unknown constants a and b can be obtained by fitting to the simulated values of a_{cc}. The KBFF simulations resulted in values of $a = 0.1164$ l/mol and $b = 0.0035$ l^2/mol^2. A fit to the experimental data gave values of $a = 0.0876$ l/mol and $b = 0.0110$ l^2/mol^2. The molar activity coefficients obtained using these values are displayed in Fig. 4. The KBFF reproduced the solution activity very well.

The salt and water partial molar volumes are displayed in Fig. 5. It is encouraging that the increase in salt partial molar volume and decrease in water partial molar volume with salt concentration were reproduced by the model. However, a slightly larger variation of salt partial molar volume with concentration was predicted. The solution density, isothermal compressibility, and relative permittivity are displayed in Fig. 6. All the observed variations with concentration were reproduced by the KBFF model. The heat of mixing is also displayed in Fig. 6. Again, the KBFF model performed well. It was also observed that the heat of mixing was a good indicator of a successful model. For instance, the experimental heat of mixing for a 2 M salt solution is 0.11 kJ/mol, compared to the KBFF value of 0.07 kJ/mol. If one

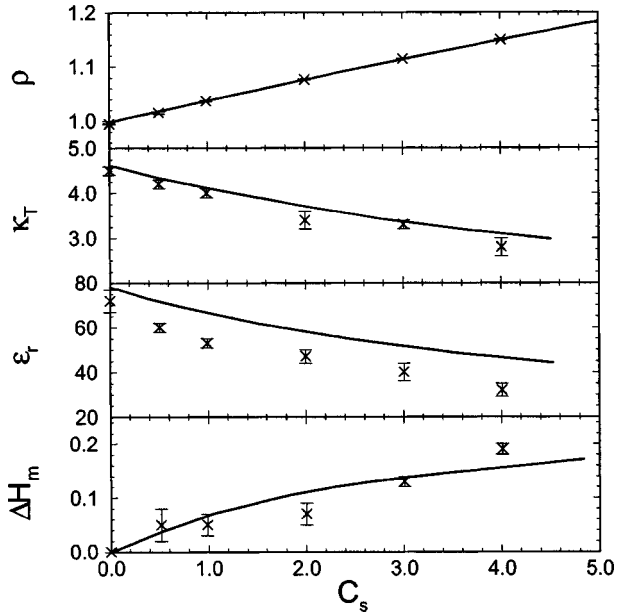

FIG. 6. Density (g/cm^3), isothermal compressibility (10^{-5} atm^{-1}), relative permittivity, and excess enthalpy of mixing (kJ/mol) as a function of molar salt concentration. Lines represent the experimental data (Refs. 18, 32, and 33) and crosses correspond to the KBFF model.

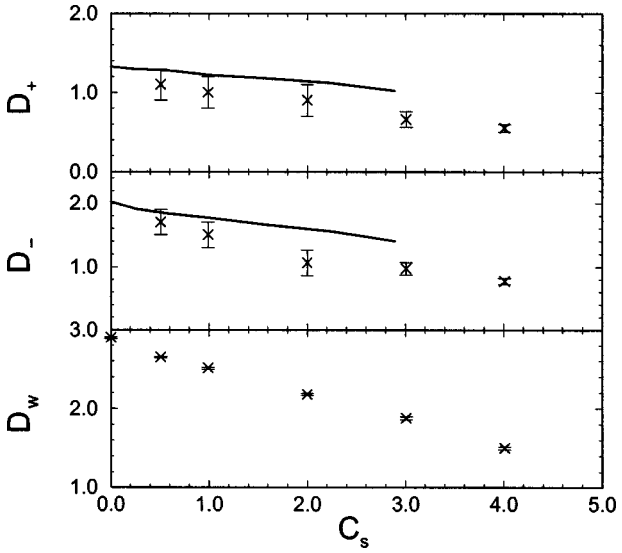

FIG. 7. Diffusion constants (10^{-9} m^2/s) as a function of molar salt concentration. Lines represent the experimental data (Ref. 31) and crosses correspond to the KBFF model.

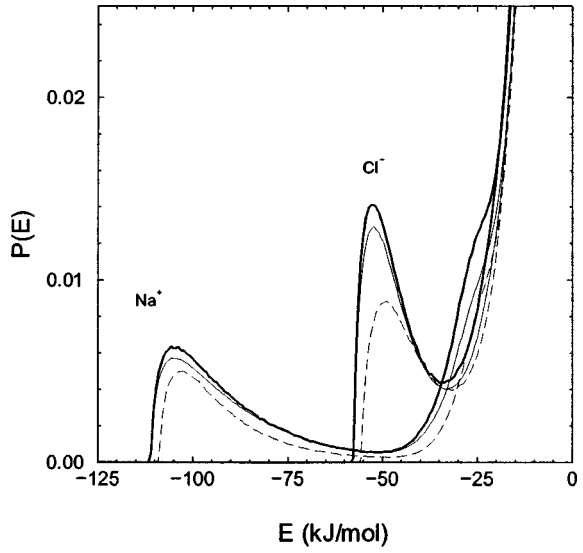

FIG. 8. Pair interaction energy probabilities between ions and water molecules. Thick and thin lines correspond to 1 M and 4 M solutions, respectively. The dashed line corresponds to a 2 M solution of the GROMOS/SPC model.

performs a simulation of the crystal using the GROMOS ion parameters a lattice energy of −817 kJ/mol is obtained, which is very similar to the KBFF result. However, the resulting heat of mixing with SPC water was 5.09 kJ/mol for a 2 M solution. This value is large and unfavorable and helps to explain why the GROMOS ions do not mix as well with water (large G_{cc} and small G_{cw}) as the KBFF ions. Furthermore, a substantial part of this increase arises from using the combination rule. Using the KBFF parameters without the 0.75 scaling of the sodium to water oxygen ε value resulted in a heat of mixing of 1.28 kJ/mol for 2 M salt, an order of magnitude too unfavorable.

The ion and water diffusion constants as a function of concentration are displayed in Fig. 7. The KBFF model slightly underestimated both ion diffusion rates. The decrease in diffusion with concentration was reproduced and the (linearly extrapolated) infinite dilution diffusion constants of 1.2 and 1.8×10^{-9} m^2/s for sodium and chloride, respectively, were in reasonable agreement with the corresponding experimental values of 1.33 and 2.03 $\times10^{-9}$ m^2/s.[31]

To further analyze the energetics of ion solvation, as described by the KBFF model, the ion-to-water pair interaction energy probability distributions were determined and are displayed in Fig. 8. The distributions highlight the strong solvation energy of the first shell water molecules surrounding sodium, with a weaker interaction energy between chloride ions and water. A comparison with the GROMOS/SPC model showed that both the sodium-to-water and chloride-to-water pair interactions were shifted to higher energies, probably as a consequence of the smaller charges on the SPC water model. This is consistent with the observed higher degree of ion self-association (lower solvation) for the GROMOS/SPC model displayed in Fig. 3 and Table IV. Examination of the average ion-to-water pair interaction energies displayed in Fig. 9 indicates an average interaction between sodium and water and chloride and water at contact of −100 and −50 kJ/mol, respectively. Furthermore, these values were independent of the concentrations studied here. The major changes as a function of concentration appeared to be for chloride-to-water pairs directly beyond the contact distance of 0.32 nm. This change was also evident in the orientation of water molecules as a function of distance from a chloride ion which is also presented in Fig. 9.

The presence of ions in solution results in screening of ion-to-ion interactions. This effect is well reproduced at low concentrations by the Debye–Hückel model.[16] However, at high concentrations the model is known to fail. In an effort to gain some insight into screening of ions in concentrated salt solutions we have determined the average total charge,

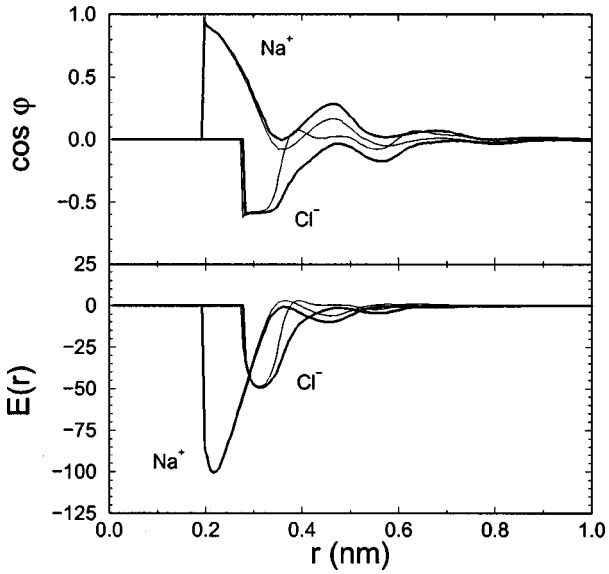

FIG. 9. The average angle between the water dipole vector and the water-to-ion intermolecular (r_o-r_i) vector (top) and the average ion–water interaction energy (kJ/mol) as a function of ion–water distance (bottom). Thick and thin lines correspond to 1 M and 4 M solutions, respectively.

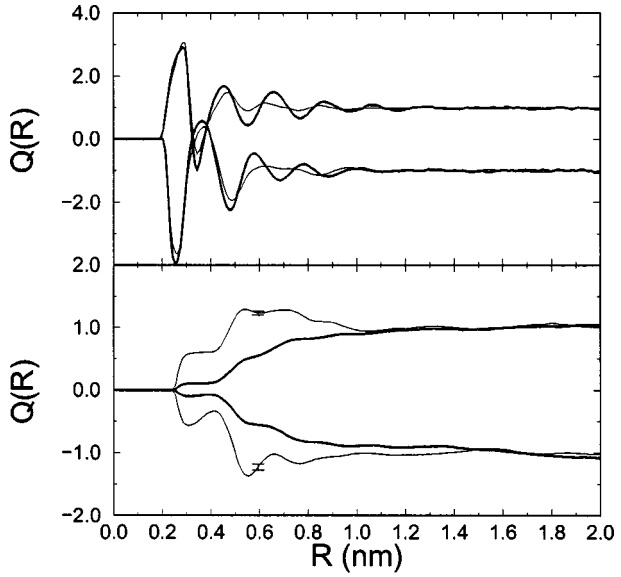

FIG. 10. The average net charge around a sodium or chloride ion as a function of distance from the ion when including all charges (top) or just other ion charges (bottom). Thick and thin lines correspond to 1 ns averages obtained from the 1 M and 4 M solutions, respectively.

$Q(R)$, contained with a sphere of radius R surrounding an ion from the KBFF simulations. The results are displayed in Fig. 10. Including all charges (ions and water atoms) produced an oscillating total charge which decreased in magnitude for higher salt concentrations.[24] The contribution of just the ions to the total charge surrounding an ion displayed less structure. Electroneutrality was achieved within 1.5 nm for the 1 M solution and 1.0 nm for the 4 M solution. This is in agreement with the larger degree of screening expected for high salt concentrations. However, it appeared that the 4 M solution resulted in an initial over compensation of ion charge (between 0.5–0.6 nm), which then decreased with distance to the limiting value.

The KBFF model has been designed to be used with the SPC/E model of water. However, many of the common protein force fields have adopted the SPC or TIP3P water models. The properties of the KBFF model with several different water models are presented in Table V for a 4 M salt solution. Not surprisingly, the best agreement was obtained for the SPC/E model. The other water models resulted in increased ion self-association and a corresponding decrease in ion-to-water association. However, the values G_{cc} remained negative and displayed potential improvement over the other salt parameters considered here. A simulation of the KBFF model without the sodium-to-water oxygen ε scaling is also presented in Table V to illustrate problems fitting the KB data without breaking the ε geometric combination rule. While the ion diffusion constants remained essentially unaffected, the value of G_{cc} increased significantly with a corresponding drop in a_{cc} to a third of the original value.

TABLE V. Comparison of the properties of a 4 M KBFF NaCl solution obtained with different water models. All simulations were performed for 2 ns at 300 K and 1 atm using 154 sodium chlorides and 1950 water molecules and the parameters from Table I. Experimental data, density from Ref. 18 and KB integrals from Ref. 9.

	SPC/E	SPC/E[a]	SPC	TIP3P	Expt.	Units
ρ	1.149	1.134	1.133	1.139	1.148	g/cm^3
C_s	4.01	3.96	3.95	3.97	4.00	mol/l
D_+	0.6	0.5	0.8	1.0		10^{-9} m^2/s
D_-	0.8	0.7	1.2	1.1		10^{-9} m^2/s
D_w	1.50	1.63	2.05	2.73		10^{-9} m^2/s
$\overline{V_s}$	24.2	26.4	23.4	23.2	22.6	cm^3/mol
$\overline{V_w}$	17.8	17.9	18.1	18.0	17.9	cm^3/mol
G_{cc}	−48	102	−18	−28	−54	cm^3/mol
G_{ww}	−18	−16	−18	−27	−18	cm^3/mol
G_{cw}	−8	−26	−10	−9	−6	cm^3/mol
a_{cc}	1.47	0.50	1.07	1.18	1.63	

[a]Simulation performed without scaling the cation water oxygen ε value.

CONCLUSIONS

A model for sodium chloride solutions has been developed which reproduces the experimentally derived Kirkwood–Buff integrals and a range of other physical and thermodynamic properties as a function of concentration. Agreement with the experimental data required a break in the normal ε geometric combining rules so as to increase the degree of solvation of the sodium ion. Only then was the excess enthalpy of mixing reproduced and the degree of ion self-association reduced to be in agreement with experiment. In our opinion, the model represents an improvement over sodium chloride parameters currently in use with common protein force fields. This is not say that the other models are not useful. That depends on the property one is interested in. Our main objective was to develop force fields for the study of preferential interactions of cosolvents with solutes in solution. In this respect, it has been shown that the activity derivative of the cosolvent solution (a_{cc}) must be correctly reproduced if a realistic measure of cosolvent-to-solute association is to be obtained.[5] The model presented here achieves that goal.

ACKNOWLEDGMENT

This material is based upon work supported by the NSF.

[1] Z. Peng, C. S. Ewig, M. Hwang, M. Waldman, and A. T. Hagler, J. Phys. Chem. A **101**, 7243 (1997).
[2] S. Weerasinghe and P. E. Smith, J. Phys. Chem. B **107**, 3891 (2003).
[3] S. Weerasinghe and P. E. Smith, J. Chem. Phys. **118**, 10663 (2003).
[4] R. Chitra and P. E. Smith, J. Chem. Phys. **115**, 5521 (2001).
[5] S. Weerasinghe and P. E. Smith, J. Chem. Phys. **118**, 5901 (2003).
[6] A. Ben-Naim, *Statistical Thermodynamics for Chemists and Biochemists* (Plenum, New York, 1992).
[7] J. G. Kirkwood and F. P. Buff, J. Chem. Phys. **19**, 774 (1951).
[8] R. Chitra and P. E. Smith, J. Chem. Phys. **114**, 426 (2001).
[9] R. Chitra and P. E. Smith, J. Phys. Chem. B **106**, 1491 (2002).
[10] S. Weerasinghe and B. M. Pettitt, Mol. Phys. **82**, 897 (1994).
[11] *Advances in Thermodynamics. Fluctuation Theory of Mixtures*, edited by E. Matteoli and G. A. Mansoori (Taylor & Francis, New York, 1990), Vol. 2.
[12] R. Chitra and P. E. Smith, J. Phys. Chem. B **105**, 11513 (2001).
[13] P. G. Kusalik and G. N. Patey, J. Chem. Phys. **86**, 5110 (1987).
[14] H. L. Friedman and P. S. Ramanathan, J. Phys. Chem. **74**, 3756 (1970).
[15] R. Behera, J. Chem. Phys. **108**, 3373 (1998).
[16] R. A. Robinson and R. H. Stokes, *Electrolyte Solutions* (Butterworths, London, 1959).
[17] O. Miyawaki, A. Saito, T. Matsuo, and K. Nakamura, Biosci., Biotechnol., Biochem. **61**, 466 (1997).

[18] P. S. Z. Rogers and K. S. Pitzer, J. Phys. Chem. Ref. Data **11**, 15 (1982).
[19] E. Matteoli and L. Lepori, J. Chem. Phys. **60**, 2856 (1984).
[20] H. J. C. Berendsen, J. P. M. Postma, W. F. van Gunsteren, A. DiNola, and J. R. Haak, J. Chem. Phys. **81**, 3684 (1984).
[21] J.-P. Ryckaert, G. Ciccotti, and H. J. C. Berendsen, J. Comput. Phys. **23**, 327 (1977).
[22] S. W. de Leeuw, J. W. Perram, and E. R. Smith, Proc. R. Soc. London, Ser. A **373**, 27 (1980).
[23] T. Darden, D. York, and L. Pedersen, J. Chem. Phys. **98**, 10089 (1993).
[24] R. Chitra and P. E. Smith, J. Phys. Chem. B **104**, 5854 (2000).
[25] M. P. Allen and D. J. Tildesley, *Computer Simulation of Liquids* (Oxford University Press, Oxford, 1987).
[26] M. Fioroni, K. Burger, A. E. Mark, and D. Roccatano, J. Phys. Chem. B **104**, 12347 (2000).
[27] W. F. van Gunsteren, S. R. Billeter, A. A. Eising, P. H. Hünenberger, P. Krüger, A. E. Mark, W. R. P. Scott, and I. G. Tironi, *Biomolecular Simulation: The GROMOS96 Manual and User Guide* (vdf Hochschulverlang, ETH Zürich, Switzerland, 1996).
[28] Y. Marcus, Chem. Rev. (Washington, D.C.) **88**, 1475 (1988).
[29] W. J. Moore, *Physical Chemistry*, 4th ed. (Prentice-Hall, New Jersey, 1972).
[30] R. S. Berry, S. A. Rice, and J. Ross, *Physical Chemistry* (Wiley, New York, 1980).
[31] H. J. V. Tyrrell and K. R. Harris, *Diffusion in Liquids* (Butterworths, London, 1984).
[32] R. Buchner, G. T. Hefter, and P. M. May, J. Phys. Chem. A **103**, 1 (1999).
[33] G. Beggerow, in *Landolt-Boernstein*, edited by K. Schaefer (Springer-Verlag, Berlin, 1976), Vol. 2, p. 89.
[34] W. R. P. Scott, P. H. Hunenberger, I. G. Tironi *et al.*, J. Phys. Chem. A **103**, 3596 (1999).
[35] W. D. Cornell, P. Cieplak, C. I. Bayly *et al.*, J. Am. Chem. Soc. **117**, 5179 (1995).
[36] A. D. MacKerell, Jr., D. Bashford, M. Bellott *et al.*, J. Phys. Chem. B **102**, 3586 (1998).
[37] H. J. C. Berendsen, J. R. Grigera, and T. P. Straatsma, J. Phys. Chem. **91**, 6269 (1987).
[38] H. J. C. Berendsen, J. P. M. Postma, W. F. van Gunsteren, and J. Hermans, in *Intermolecular Forces*, edited by B. Pullman (Reidel, Dordrecht, 1981), pp. 331–342.
[39] W. L. Jorgensen, J. Chandrasekhar, J. D. Madura, R. W. Impey, and M. L. Klein, J. Chem. Phys. **79**, 926 (1983).